Int. J. Electrochem. Sci., 15 **(2020)** 5089 – 5101, doi: 10.20964/2020.06.87

International Journal of
ELECTROCHEMICAL
SCIENCE
www.electrochemsci.org

Pretreatment by Ultrasonic-Assisted Solvent Dissolution and Electrochemical Performance of Recycled $LiNi_{0.5}Co_{0.2}Mn_{0.3}O_2$ Electrode Waste Material

Shuang Li, Hualing Tian, Zhi Su[*]

College of Chemistry and Chemical Engineering, Xinjiang Normal University, Urumqi, 830054 Xinjiang, China
[*]E-mail: suzhixj@sina.com

Received: 8 November 2019 / *Accepted:* 9 January 2020 / *Published:* 10 May 2020

The key to electrode waste $LiNi_{0.5}Co_{0.2}Mn_{0.3}O_2$ recycling is to effectively separate the cathode material from the metal Al foil for increasing the recovery rate. The method described herein utilizes the compatibility between an organic solvent and polyvinylidene fluoride (PVDF), ultrasonic-induced cavitation and convection effects, and the decomposition temperature of PVDF. The duration of ultrasonication, type of organic solvent, ratio of organic solvent to cathode material, stirring temperature, stirring time, sequence of ultrasonication and stirring, and calcination temperature were explored for determining optimum conditions. Thus, it was determined that the optimum peeling efficiency was approximately 93 %.The cathode material pretreated by the organic solvent was calcined, and the PVDF binder was effectively removed by calcination at 600 °C. Calcination at 800 °C yielded a cathode material with a suitable lamellar structure and the highest electrochemical performance, with an initial specific discharge capacity of 164.2 mAh g^{-1}. The specific discharge capacity was 132.4 mAh g^{-1} after 50 charge-discharge cycles, which translates to a capacity retention rate of 80.6 %.

Keywords: $LiNi_{0.5}Co_{0.2}Mn_{0.3}$; Recycling and utilization; Solvent solution method; Electrode Waste; ultrasonic

1. INTRODUCTION

With the continuous advancement of science, batteries have become an important commodity, and the traditional nickel-cadmium and lead-acid batteries are unable to meet the ever-increasing requirements for power supplies. Lithium, on the other hand, has a lower electrode potential and specific gravity and higher theoretical specific capacity. Since their introduction by Sony in 1991 [1], lithium-ion batteries (LIBs) have been extensively utilized for their portability in applications ranging

from microelectronics, mobile phones, and computers to large-scale power storage devices such as renewable energy systems [2]. With the development of new energy vehicles and the hybrid electric vehicle industry [3], LIBs have become appealing, owing to their high energy densities and cycle stabilities, lack of memory effects, high charging rates, and operating temperature [4-5]. As the main electric vehicle power supply [6-7], it is estimated that the global annual production of LIBs increased by 800 % between 2000 and 2010 [8]. LIBs have a total service life of approximately 1000 charge-discharge cycles (1-3 years) [9-10]. Therefore, the demand for LIBs is increasing.

In industrial production, electrode waste is generated in addition to used LIBs. This waste has not been assembled into a battery, come into contact with the electrolyte, or been subjected to charge-discharge tests, and hence, has a relatively complete structure. If the remaining electrode waste is landfilled or dumped, it will affect the soil and surrounding ecosystems [11-12]. At the same time, the cost of LIBs will continue to gradually increase due to the increasing shortage of energy resources. Therefore, from the perspective of environmental protection and economics, the recovery of electrode waste generated during the production of LIBs is of great significance [13].

The LIB is composed of a cathode, current collector, anode, electrolyte, and separator, where the active cathode material is a lithium transition metal oxide [14]. Removing the cathode coating composed of the active material, organic binder, and conductive agent from the Al foil is the main goal of recycling [15]. The binder accounts for only approximately 1 % of a complete battery [16]. In an LIB system of cathode materials, such as lithium iron phosphate and ternary material battery, oil-based binders are often used, the main components of which are polyvinylidene fluoride (PVDF) copolymers and homopolymers. Therefore, to effectively improve the stripping efficiency of the cathode material, the removal of PVDF is important. Common methods for the pretreatment of used batteries include high-temperature treatments, organic solvent methods, lye dissolution, and ultrasonic-assisted methods [17-18].

High-temperature treatments are generally performed above 500 °C, which will produce more harmful gases [19]; further, alkaline solutions such as NaOH will generate a large amount of alkaline wastewater [20].The organic solvent method exploits similar compatibility between two compounds to dissolve PVDF. However, because there is a strong bonding force between the cathode material and metal foil, it is difficult to achieve good results with a single pretreatment method to separate the aluminum foil from the cathode material.

In this study, an organic solvent, in combination with ultrasonic-assisted solvent dissolution and high-temperature calcination, was employed to explore the optimal stripping conditions of the cathode material (NCM523) on Al foil in electrode waste and the removal efficiency of PVDF. The experimental results indicated that the cathode material could effectively peel off from the Al foil and the regenerated $LiNi_{0.5}Co_{0.2}Mn_{0.3}O_2$ had good electrochemical performance, thereby proving the feasibility of electrode waste recovery and the effectiveness of this approach.

2. EXPERIMENTAL

2.1 Materials and reagents

The electrode waste was provided by China dongguan changmei renewable resources recycling co. LTD, N-N-dimethylacetamide (DMAC), N-N-dimethylformamide (DMF), N-methyl-2-pyrrolidone (NMP), and ethanol were used as analytical reagents.

2.2 Experimental procedure

The peeling efficiency (PE) was influenced by several elements, such as the type of organic solvent, the sequence of ultrasonication and stirring, the solid-liquid ratio (S:L), temperature and time for stirring, and duration of ultrasonication.

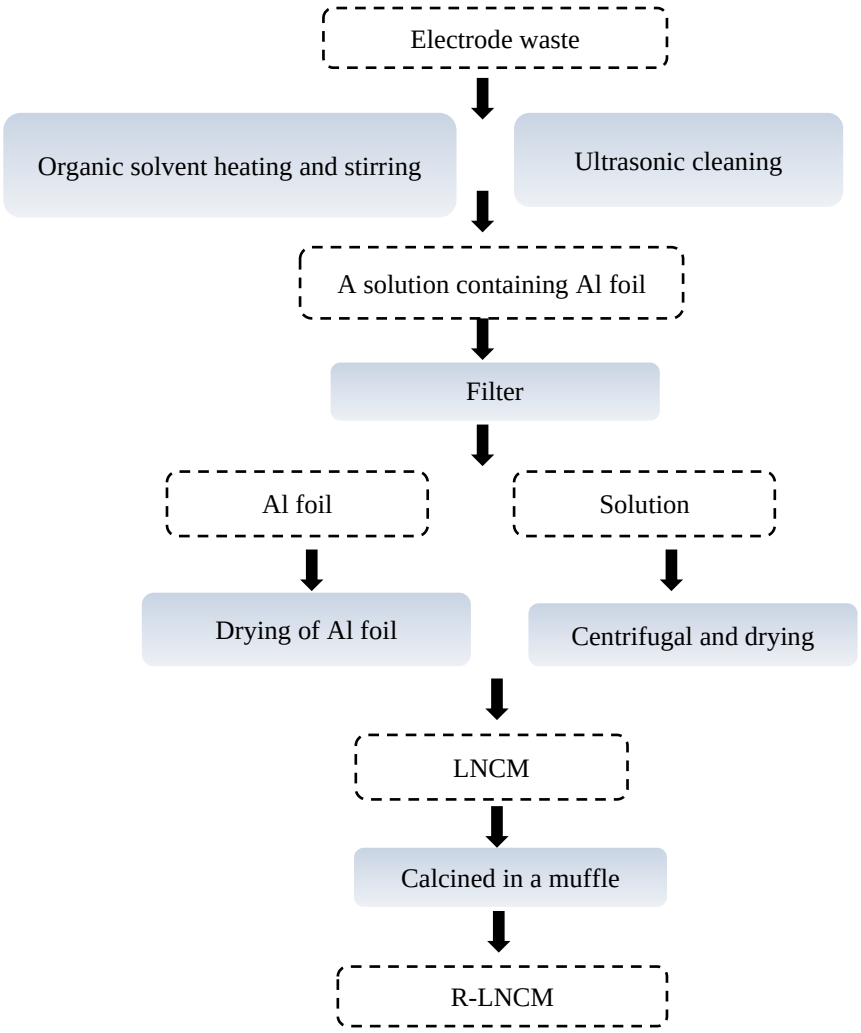

Figure 1. Flow chart of electrode waste recovery

Therefore, we conducted a single-factor variable experiment to explore the best conditions for NCM523 stripping from Al foil. The complete recovery process is shown in Figure 1. In the pre-

processing phase, the electrode waste was cut into a rectangular strip and stirred on a magnetic stirrer with different organic solvents in a 50 mL beaker at 60 °C for 30 min; the sequence followed here was stirring followed by ultrasonication. S:L was 1:10 g mL^{-1}, the duration of ultrasonication was 30 min, the Al foil was separated from the solution by a vacuum pump and dried at 80 °C for 12 h, and the mass of the foil was recorded to calculate PE. For comparison, the sequence was reversed (ultrasonication followed by stirring). When the optimum sequence was determined, we investigated PE when the temperature range was 20-70 °C, stirring time was 30-90 min, S:L was 1:10-1:40 g mL^{-1}, and duration of ultrasonication was 30-150 min. The filtrate was centrifuged and the precipitate was washed with distilled water for three times. The precipitate was then dried in an oven at 80 °C and labeled as LNCM. The LNCM was calcined in a muffle furnace at 500-900 °C, and the calcined material was labeled as R-LNCM.

PE was calculated by Eq (1)

$$PE=\frac{m1-m2}{m1}\times 100\% \quad (1)$$

Where PE is the peeling efficiency (%); and *m1* and *m2* are the masses of the materials with NCM523 and Al foil, respectively (g).

2.3 Sample characterization

The crystal structures of the samples were examined by X-ray diffraction (XRD, Bruker D2), and the peak intensities were analyzed using Jade software. Infrared spectra were acquired via Fourier transform infrared (FTIR) spectroscopy (Tensor 27, Bruker, KBr pellet), and the surface topography of the material was examined by scanning electron microscopy (SEM, Zeissm, 5-30 kV)

2.4 Electrochemical performance test

To analyze the electrochemical performance of the calcined cathode material, 80 % active cathode material, 10 % acetylene black, and 10 % PVDF were weighed and combined with a NMP solution. The mixture was ground, evenly applied to an Al foil, and dried in a vacuum oven at 110 °C for 12 h. The pole piece was punched with a 12 mm-diameter belt. A CR2025 coin-cell battery was assembled in a Ar-protected vacuum glove box using Li foil as a counter electrode, Celgard 2400 as the separator, and 1 M $LiPF_6$ in ethylene carbonate: dimethyl carbonate: ethyl methyl carbonate(1:1:1, v/v/v) as the electrolyte. A CT2001A-type Land battery test system was used to perform constant-current charge-discharge cycling tests in a voltage range of 2.75-4.5 V. Electrochemical impedance spectroscopy (EIS, frequency = 0.01 Hz to 0.1 MHz) and cyclic voltammetry (CV, scan rate = 0.1 mV s^{-1}) were performed on an electrochemical workstation (Chenhua, CHI 650D); both experiments were performed in the range of 2.75-4.5 V.

3. RESULTS AND DISCUSSION

3.1 Exploration of optimal conditions for pretreatment of electrode waste

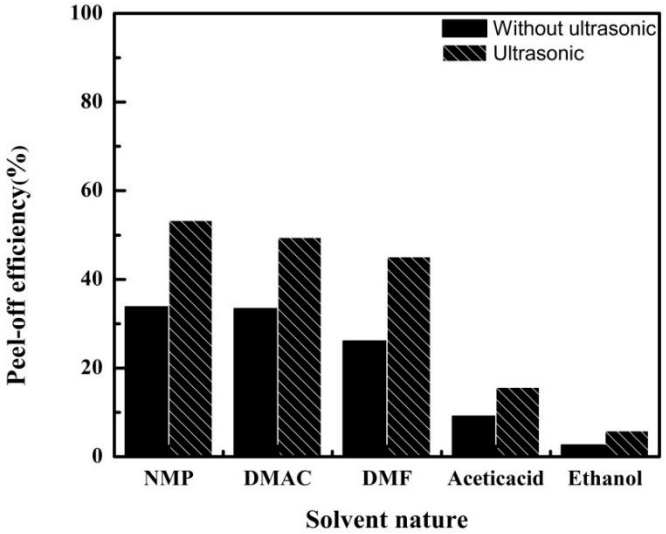

Figure 2. Effect of different solvents on material peel-off efficiency.

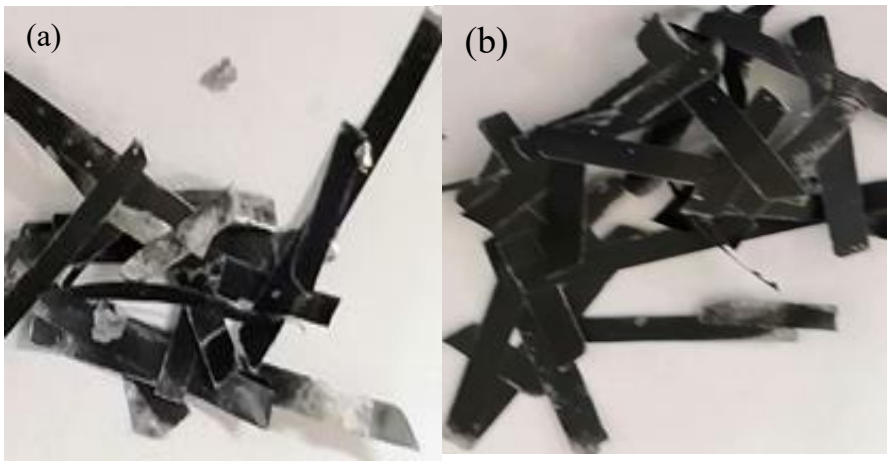

Figure 3. Effect of ultrasound and stirring on peeling-off efficiency in different orders (a) Stirring before ultrasound (b) Ultrasound before stirring.

As shown in Figure 2, ultrasonic assistance increased the PE of NCM523 1.75-fold with an S:L of 1:10 g mL^{-1} , ultrasonication duration of 30 min, stirring time of 30 min, and stirring temperature of 60 °C. This is due to the effect of ultrasonic waves on the convective motion of the solvent, as well as the cavitation effect of the ultrasonic waves [21-22]. The PE of various organic solvents decreased in the order NMP > DMAC > DMF > acetic acid > ethanol. Under the same conditions, the PE of NCM523 treated by stirring followed by ultrasonication was 1.16-fold that obtained by following the reverse sequence (Figure 3). This may be because the heating and stirring first dissolve a large amount

of NCM523 coated on the aluminum foil, which enables a higher ultrasonication performance. The optimum peel-off conditions for NCM523 in the NMP solvent were discussed using the same control variable method via stirring followed by ultrasonication.

The effects of time and temperature with stirring on the PE are shown in Figure 4 (a-b). For a stirring temperature of 60 °C and stirring time of 60 min, PEs were 74.6 % and 62 %, respectively. From Figure 4 (c-d), the PEs had the highest values of 69.3 % and 75 %, respectively, when the influencing factors were S:L and ultrasound duration, respectively.

Therefore, the optimum conditions for the pretreatment of the cathode material were determined as follows: NMP as the solvent, stirring before ultrasonication, stirring time of 60 min, stirring temperature of 60 °C, S:L (NCM523: NMP) of 1:30 g mL^{-1}, and considering lower costs and energy consumption, an ultrasonic duration of 120 min. As shown in Figure 5, electrode waste can be effectively peeled off from aluminum foil under the optimal conditions.

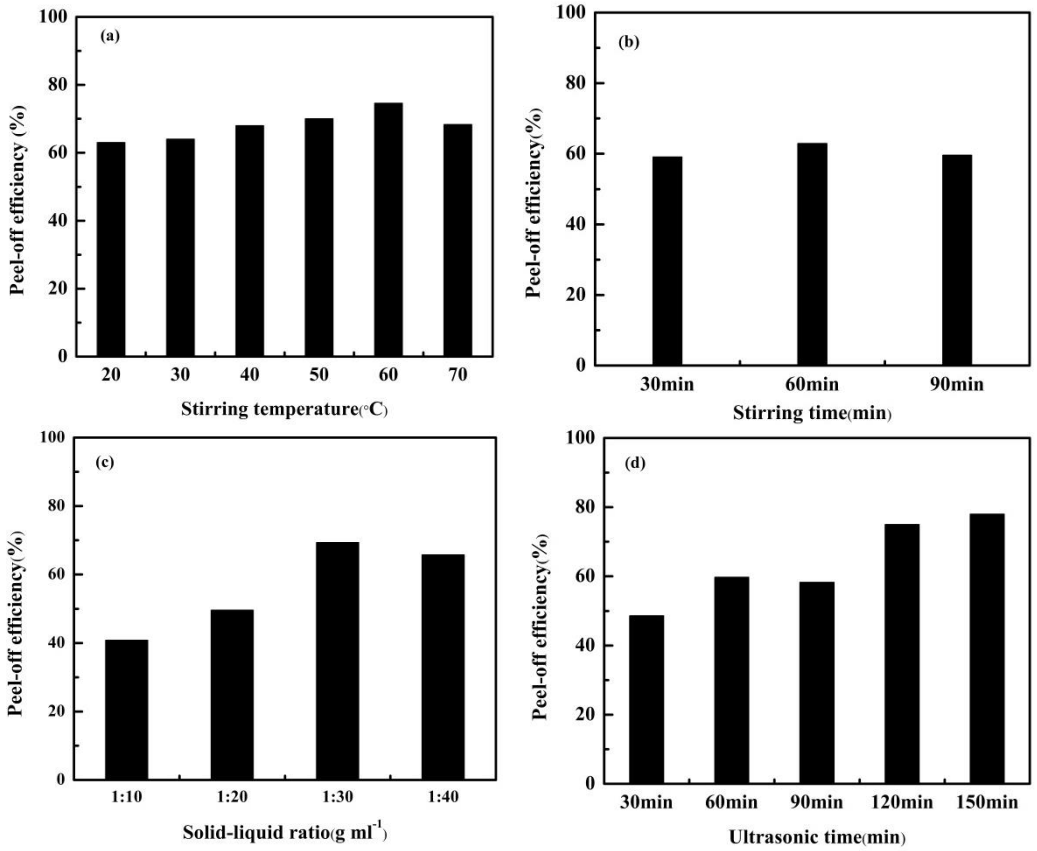

Figure 4. Effect of different conditions on peeling-off efficiency (a) Stirring temperature (b) Stirring time (c) S:L ratio (d) ultrasound time.

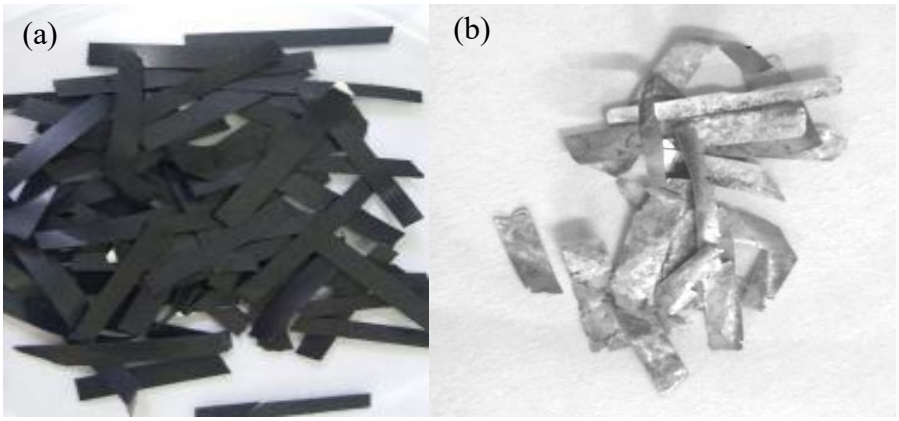

Figure 5. Effect of cathode material under optimal conditions (a) Before treatment (b) After treatment.

Figure 6 shows distinct PVDF characteristic peaks at 2067, 2814, 1589, 1421, 1161, and 835 cm^{-1} in the FTIR spectrum of NCM523, indicating that it contained PVDF. These characteristic PVDF absorption peaks in the LNCM spectrum exhibited distinctly decreased intensity compared with those in the NCM523 spectrum, demonstrating that PVDF was effectively removed under the dual action of NMP heating and ultrasonic cleaning. The characteristic PVDF absorption peaks were still present in the spectrum of R-LNCM calcined at 500 °C, signifying that a small amount of residual PVDF remained. In contrast, in the infrared spectrum of R-LNCM calcined at 600 °C, except for a peak corresponding to water at 3710 cm^{-1}, no PVDF features were observed, indicating that PVDF can be removed by calcination at 600 °C after heating and stirring with an organic solvent.

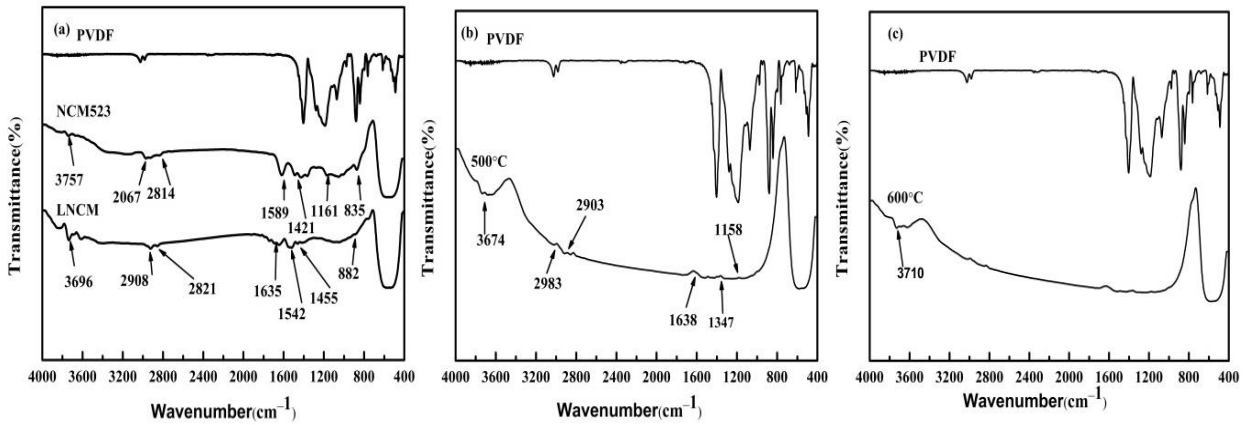

Figure 6. The IR spectra of the (a) PVDF, NCM523, LNCM and R-LNCM calcined at (b) 500°C and (c) 600°C.

3.2 Electrochemical performance of regenerated electrode materials

The R-LNCM samples were calcined in the range of 500-900 °C for 3 h. The XRD patterns and the splitting of $I_{(018)}/I_{(110)}$ and $I_{(006)}/I_{(012)}$ are shown in Figure 7, indicating that R-LNCM and NCM523 had a layered hexagonal α-$NaFeO_2$ structure, and a carbon peak was present in the NCM523 and in

that of the material calcined at 500 °C. If the ratio of $I_{(003)}/I_{(104)}$ is less than 1.2, the degree of cation mixing is small [23], and the peak intensity ratio of $I_{(003)}/I_{(104)}$ calcined at 800 °C was 1.24 (Table 1), which reaches the highest in samples calcined at 700, 800, and 900 °C, indicating that the sample had the smallest degree of cation mixing. The formation structure of the hexagonal layered structure is reflected by the value of *c/a* [24], the maximum *c/a* value of the sample calcined at 800 °C was 5.0273, which was beneficial to electrochemical performance (Table 1).

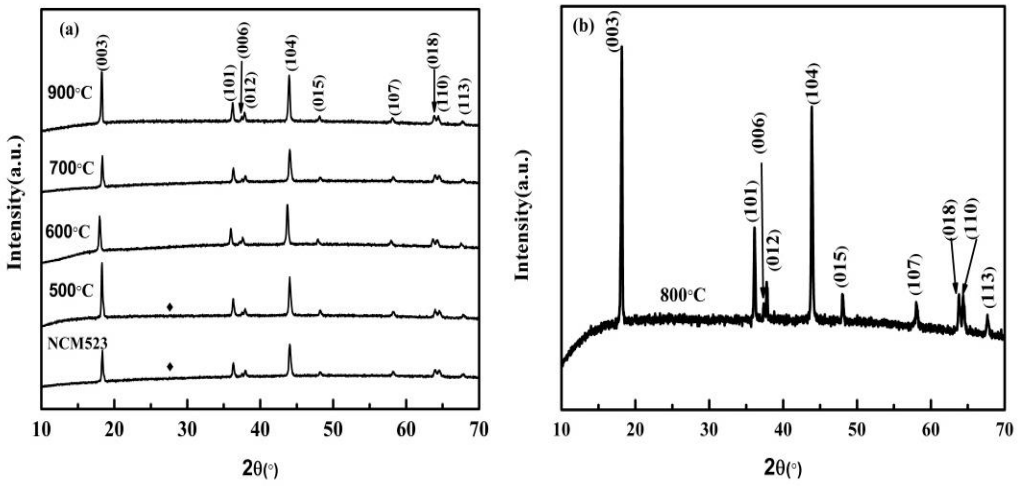

Figure 7. The XRD pattern of NCM523 and R-LNCM (a,b).

Table 1. Crystal cell parameters of R-LNCM at different calcining temperatures.

Calcination temperature (°C)	a (Å)	c (Å)	Volume (Å^3)	*c/a*	$I_{(003)}/I_{(004)}$
700	2.8960	14.2131	119.2026	4.9078	1.05
800	2.8712	14.4346	118.9958	5.0273	1.24
900	2.8954	14.2401	119.3796	4.9184	0.87

Figure 8 shows the initial charging and discharging curves of R-LNCM at different temperatures and the cycling performance at 0.2 C between 2.5 and 4.5 V. The specific values are shown in Table 2. The initial charge capacities of R-LNCM were 168.4, 156, 161.3, 167, and 189 mAh g^{-1}; initial discharge capacities were 154.5, 153.1, 154.9, 164.2, and 149.8 mAh g^{-1}, respectively; and initial coulombic efficiencies at 500, 600, 700, 800, and 900 °C were 91.7, 98.1, 96, 98.3, and 79.2 %, respectively. After 50 cycles under the same test conditions, discharge capacities of 105.9, 95, 116.7, 132.4, and 106.6 mAh g^{-1} were obtained, and the capacity retention rates were 68.5, 62, 75.3, 80.6, and 71.1 %, respectively. Therefore, the sample calcined at 800 °C had the best electrochemical performance.

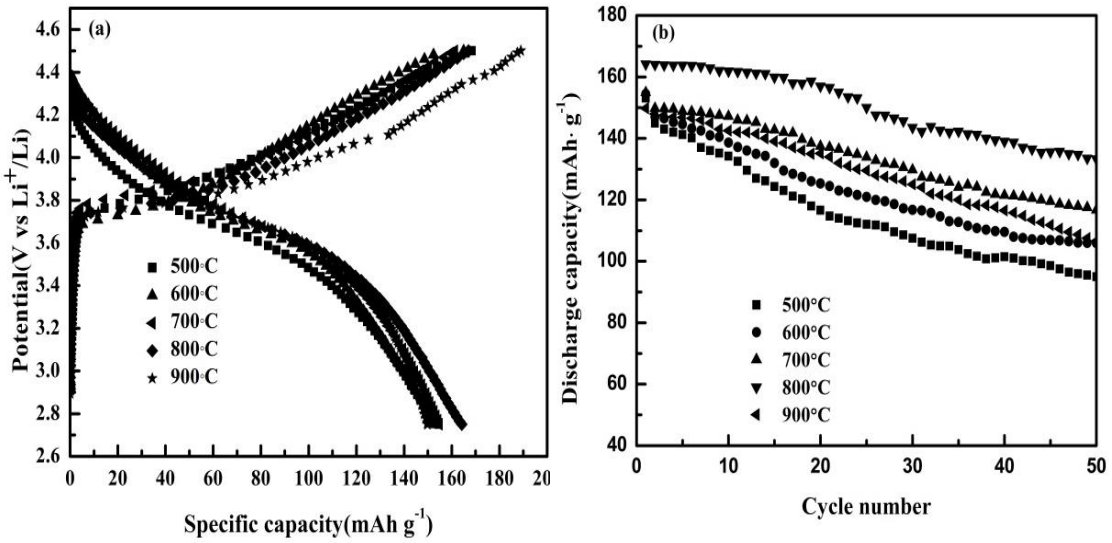

Figure 8. Initial charge-discharge curves at different temperatures and cycling performances of the R-LNCM at 0.2 C between 2.75-4.5 V (a,b).

Table 2. Initial charge-discharge Coulombic efficiency and Capacity retention rate of R-LNCM.

Calcination temperature (°C)	Initial charge capacity (mAh g^{-1})	Initial discharge capacity (mAh g^{-1})	Discharge capacity after 50 cycles (mAh g^{-1})	Initial coulombic efficiency (%)	Capacity retention (%)
500	168.4	154.5	105.9	91.7	68.5
600	156.0	153.1	95.0	98.1	62.0
700	161.3	154.9	116.7	96.0	75.3
800	167.0	164.2	132.4	98.3	80.6
900	189.0	149.8	106.6	79.2	71.1

EIS is often conducted to explore the electrochemical mechanism, which consists of several parts. The semicircular portion in the high- frequency region, termed "charge transfer impedance" (Rct), is used to characterize the difficulty of charge transfer. The impedance of a solution is indicated by the intercept of the real axis (Re), and the diffusion ability of Li^+ is represented by the slash in the low- frequency region, termed "Warburg impedance" (Zw).The charge transfer resistance of R-LNCM calcined at 800 °C was minimum at ~69 Ω, as shown in Figure 9 and the results showed that the electrochemical performance of R-LNCM sample was the best after calcined at 800 °C.

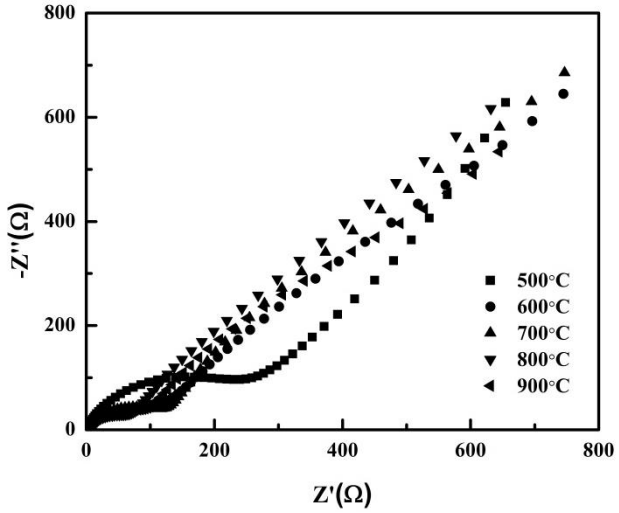

Figure 9. EIS curves of R-LNCM calcined at 500, 600, 700, 800 and 900 °C.

Figure 10 shows the CV curves for R-LNCM, obtained at a scan rate of 0.1 mV s^{-1} from 2.5 to 4.75 V. There is a distinct oxidation peak at approximately 3.9 V, with the corresponding reduction peak at 3.56 V associated with the redox reaction of Ni^{2+}/Ni^{4+}. The difference between them is 0.34 V, indicating that the material has high polarization degree and poor circulation performance when charging and discharging.

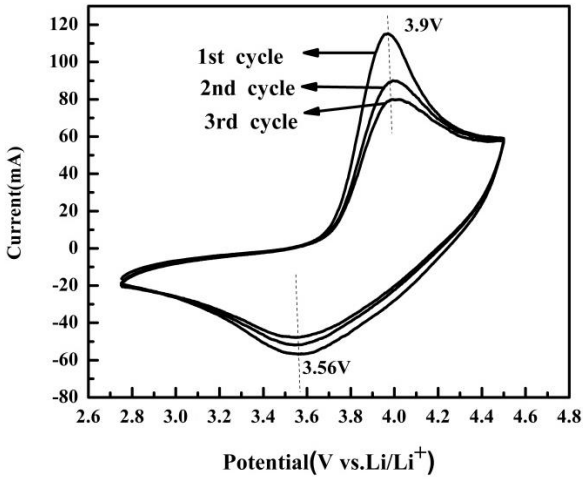

Figure 10. CV curves of R-LNCM calcined at 800 °C.

The SEM images of NCM523 covered by a layer of PVDF are shown in Figure 11. When the recovered cathode material was calcined at 700 °C, the morphology of the cathode material was irregular and the crystallinity was poor. When the calcined temperature was 900 °C, the cathode material presented an irregular and partially agglomerated spherical structure. At the same time, the

increase of particle size was also obvious, which would increase the internal impedance of the battery. In contrast, when the calcination temperature was 800 °C, the cathode material exhibited a regular shape, and the particles were evenly distributed without distinct agglomeration; further, a small particle material was formed on the surface. This enabled enhanced contact with the electrolyte, thereby contributing to the improved electrochemical performance, as evinced by the results.

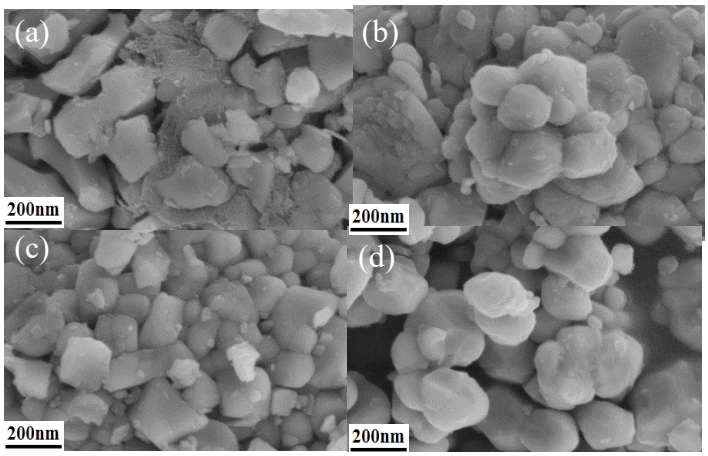

Figure 11. SEM image of cathode material after different conditions (a) NCM523 (b) 700 °C (c) 800 °C (d) 900 °C.

Yan et al. [25] dissolved waste $LiNi_{0.5}Co_{0.2}Mn_{0.3}O_2$ powder by adding H_2O_2 to sulfuric acid, then obtained the precursor $Ni_{0.5}Co_{0.2}Mn_{0.3}(OH)_2$ with an amorphous structure by co-precipitation, and prepared the precursor system with lithium carbonate. Both were calcined in air atmosphere for 20 h at 800 °C, with an initial discharge capacity of 140 mAh g^{-1} and a current density of 100 mA g^{-1}. Li et al. [26] used a molecular sieve to separate Al foil and the cathode material to achieve a powder state with a shredder.

Table 3. Comparison of electrochemical properties of regenerated cathode material $LiNi_{0.5}Co_{0.2}Mn_{0.3}$.

Author	Material	Initial discharge capacity (mAh g^{-1})	current density
Yan et al. [25]	$LiNi_{0.5}Co_{0.2}Mn_{0.3}O_2$	140	100 mA g^{-1}
Li et al. [26]	$LiNi_{0.5}Co_{0.2}Mn_{0.3}O_2$	161.25	0.1 C
Shi et al. [27]	$LiNi_{0.5}Co_{0.2}Mn_{0.3}O_2$	149.3	1 C
regenerated material of this work	$LiNi_{0.5}Co_{0.2}Mn_{0.3}O_2$	164.2	0.2 C

The separated cathode material was pre-sintered at 550 °C, followed by the addition of $LiOH{\bullet}H_2O$ and calcination at 850 °C for 12 h. Thus, the initial discharge specific capacity of the cathode material was tuned to reach 161.25 mAh g^{-1} at 0.1 C. Shi et al. [27] combined environmental pressure and a low-temperature molten salt reaction with a short thermal annealing reaction to

regenerate the cathode material $LiNi_{0.5}Co_{0.2}Mn_{0.3}O_2$. Thus, the regenerated cathode material exhibited a discharge capacity of 149.3 mAh g^{-1} at 1 C. The above experimental methods have some shortcomings in terms of recovery cost and environmental protection. The recycled cathode materials in this study and the above results are listed in Table 3. The solvent - dissolved cathode material calcined directly has better discharge specific capacity and electrochemical performance, and avoids complex stripping method and regeneration procedure.

4. CONCLUSIONS

In this study, the optimum conditions for the pretreatment of electrode waste by a solvent dissolution method were investigated in detail. Under the best conditions of pretreatment, the PE of the cathode material with NMP reached 93 %. The cathode material after centrifugation in an organic solvent was calcined at different temperatures. The FTIR spectrum indicated that the electrode waste contained PVDF, which was effectively removed by calcination at 600 °C. The samples were calcined at 800 °C, and the capacity retention rate reached 80.6 % after 50 cycles; however, the cycling stability requires further improvement. The research method employed herein avoids complicated separation methods for valuable metals, and can efficiently recover electrode waste. Our follow-up research will focus on the exploration of green solvents and the development of more environmentally friendly methods.

ACKNOWLEDGMENTS
The study was supported by the tianshan cedar technology innovation leading talent project of Xinjiang (2018XS03)

References

1. Y. Yoda, K. Kubota, H. Isozumi, T. Horiba and S. Komaba, *ACS Appl. Mater. Interfaces*, 10 (2018) 10986.
2. Y. Zhao, M. Noori and O. Tatari, *Energy*, 120 (2017) 608.
3. P. Liu, L. Xiao, Y. Tang, Y. Zhu, H. Chen and Y. Chen, *Vacuum*, 156 (2018) 317.
4. T. Sieber, J. Ducke, A. Rietig, T. Langner and J. Acker, *Nanomater.*, 9 (2019) 246.
5. D.A. Bertuol, C.M. Machado, M.L. Silva, C.O. Calgaro, G.L. Dotto and E.H. Tanabe, *Waste Manage.*, 51 (2016) 245.
6. X. Chen, B. Fan, L. Xu, T. Zhou and J. Kong, *J. Cleaner Prod.*, 112 (2016) 3562.
7. X. Chen and T. Zhou, *Waste Manage. Res.*, 32 (2014) 1083.
8. X. Zhang, Q. Xue, L. Li, E. Fan, F. Wu and R. Chen, *ACS Sustainable Chem. Eng.*, 4 (2016) 7041.
9. R. Balbierer, R. Gordon, S. Schuhmann, N. Willenbacher, H. Nirschl and G. Guthausen, *J. Mater. Sci.*, 54 (2019) 5682.
10. W. Chen and H.J. Ho, *Metals*, 8 (2018) 321.
11. Y. Nishi, *J. Power Sources*, 100 (2001) 101.
12. L. Li, J. Lu, Y. Ren, X. Zhang, R. Chen, F. Wu and K. Amine, *J. Power Sources*, 218 (2012) 21.
13. A. Changes and B. Pospiech, *J. Chem. Technol. Biotechnol.*, 88 (2013) 1191.
14. M. Jo, S. Park, J. Song and K. Kwon, *J. Alloys Compd.*, 764 (2018) 112.

15. T.Sieber, J. Ducke, A. Rietig, T. Langner and J. Acker, *Nanomater.*, 9 (2019) 246.
16. J. Li, L. Christensen, M.N. Obrovac, K.C. Hewitt and J.R. Dahn, *J. Electrochem. Soc.*, 155 (2018) A234.
17. Y. Guo, F. Li, H. Zhu, G. Li, J. Huang and W. He, *Waste Manage.*, 51 (2016) 227.
18. W. Gao, C. Liu, H. Cao, X. Zheng, X. Lin, H. Wang, Y. Zhang and Z. Sun, *Waste Manage.*, 75 (2018) 477.
19. T.G. Fonseca, M. Auguste, F. Riberio, C. Cardoso, N.C. Mestre, D.M.S. Abessa and M.J. Bebianno, *Sci. Total Environ.*, 636 (2018) 798.
20. Y. Yang, G. Huang, S. Xu, Y. He and X. Liu, *Hydrometallurgy*, 165 (2016) 390.
21. N.A. Oz and C.C. Yarimtepe, *Waste Manage.*, 34 (2014) 1165.
22. L. He, S. Sun, X. Song and J. Yu, *Waste Manage.*, 46 (2015) 523.
23. L. Zhang, B. Wu, N. Li, D. Mu, C. Zhang and F. Wu, *J. Power Sources*, 240 (2013) 644.
24. S.W. Oh, S.H. Park, C.W. Park and Y.K. Sun, *Solid State Ionics*, 171 (2004) 167.
25. S. Yan, R. Wang, C. Shao, Z. Tong, T. Li, L. Yuan, G. Sheng and K. Xu, *J. Power Sources*, 440 (2019) 227140.
26. J. Li, L. Hu, H. Zhou, L. Wang, B. Zhai, S. Yang, P. Meng and R. Hu, *J. Mater. Sci.: Mater. Electron.*, 29 (2018) 17661.
27. Y. Shi, M. Zhang, Y.S. Meng and Z. Chen, *Adv. Energy Mater.*, 9 (2019) 1900454.